Proceedings of Innovative Research and Industrial Dialogue'16, pp. 161-162 (May 2017)

Effect of surfactant on the surface integrity of stainless steel using EDM

P.J.Liew[1,*], Z.Nurlishafiqa[1], S.H.Amira[1]

[1] Department of Manufacturing Process, Faculty of Manufacturing Engineering, Universiti Teknikal Malaysia Melaka, Hang Tuah Jaya, 76100 Durian Tunggal, Melaka, Malaysia

[*]Corresponding e-mail: payjun@utem.edu.my

Keywords: Surfactant; Surface Integrity; Electrical Discharge Machining (EDM)

ABSTRACT – This paper investigates the effect of surfactant on the surface integrity of stainless steel using electrical discharge machining (EDM). The surfactants Gam Arabic (GA) and PolyvinylPyrrolidone (PVP) were mixed together with deionized water (DIW) and carbon nanofiber (CNF) as the dielectric fluid by using ultrasonic homogenizer equipment. The results show that the effects of both surfactants towards the hardness of machined surface were insignificant. However, by using PVP surfactant, lowest recast layer thickness can be obtained compared to dielectric fluid with GA surfactant and without surfactant.

1. INTRODUCTION

Electrical discharge machining (EDM) has been extensively used in the mould and dies industries. This process is essentially a metal removal process that uses electrical discharge to cause melting and vaporization of materials from the workpiece [1]. Nowadays, many researchers are interested to investigate the use of powders in dielectric fluid to facilitate material removal rate (MRR), reduce the electrode wear ratio (EWR) and improve the surface integrity of the workpiece [2-4]. Commonly, for powder-mixed EDM, the conventional electrodes are used with suspended powder particles in the dielectric fluid to obtain improvement in the surface of materials. These powder particles help to improve the sparking efficiency during EDM process [5]. However, agglomeration of powder still remains a problem in powder-mixed EDM.

Some of the previous researchers suggested using the surfactant to reduce the agglomeration of powder. For example, Wu et al. investigated the influence of surfactant on the characteristics of EDM process on mold steel (SKD61). The results show that after the addition of surfactant Span 20 (30 g/L) to the dielectric fluid with proper working parameters, the conductivity of dielectric was increased, thus increased the EDM machining efficiency. Besides that, the surfactant could improve the surface quality of workpiece quite effectively by increasing the MRR and decreasing EWR, especially in mid-finish machining and finish machining [6]. However, up to date, the studies on the effect of surfactant in powder-mixed EDM are still scarce.

Therefore, this paper intends to investigate the effect of different types of surfactants on the surface integrity of AISI 304 stainless steel using EDM.

2. EXPERIMENTAL METHODS

2.1 Machining conditions

Copper rod with 6 mm diameter was used as tool electrode. Before the EDM of stainless steel, the tool electrode tip was dressed by using grinding machine in order to improve it accuracy. The electrode dressing was also performed after each EDM cycle because the tip electrode, especially the corner, will wear. The workpiece material used in the experiment was AISI 304 stainless steel plate with dimension 40mm (width) x 50mm (length) x 5mm (thickness).

The dielectric fluid used was deionized water, which is very low cost dielectric fluid. In order to prepare the mixed dielectric, the required amounts of surfactants and deionized water were measured separately before being mixed together and homogenized in a mixer for 35 minutes using ultrasonic homogenizer equipment. After that, CNF was added into the mixture and being mixed together again for 1 hour. Surfactant was introduced into the mixture of deionized water and CNF to ensure these fibers well dispersed in the dielectric fluid. Gam Arabic (GA) and PolyvinylPyrrolidone (PVP) were used as the surfactants in this study. Table 1 shows the weight ratio of CNF with surfactant for specified volume of deionized water. Table 2 illustrates the experimental conditions in this study.

Table 1 Weight ratio of CNF with surfactant for 500ml deionized water

Weight ratio of surfactant : Carbon nanofiber (CNF)	CNF (g)	Surfactant (g)
1:1	0.75	0.75
1:2	0.75	1.50
1:3	0.60	2.25

Table 2 Experimental conditions

Workpiece material	AISI 304 stainless steel
Electrode material	Copper
Polarity	Negative (electrode)
Voltage	22V
Peak current	5A
Pulse on-time	80μs
Pulse off-time	40μs
Machining time	10 min

2.2 *Measurement and evaluation*

Surface hardness of the workpiece was measured using Vickers hardness testing. The hardness testing was repeated for 3 times at different points in each sample. After that, the recast layer thickness (RLT) was measured using metallurgical microscope under a magnification of 500X. The RLT was measured at 5 different locations for each cross-section specimen and the average value was calculated.

3. RESULTS AND DISCUSSION

3.1 *Surface hardness*

Figure 1 illustrates the comparison of surface hardness of workpiece when using different types of dielectric fluids against the concentration of CNF to surfactant (CNF: surfactant). It can be observed that the addition of surfactants in dielectric fluid shows insignificant effect against the hardness of workpiece after EDM machining. This condition happened might be due to the same cooling rate after machining process and this may leads to the same hardness result. During cooling process, the machined workpiece surfaces were freeze and turn into martensitic structures. The addition of surfactants only helps to improve the dispersion of CNF in dielectric fluid, but not affects to the cooling rate after machining process.

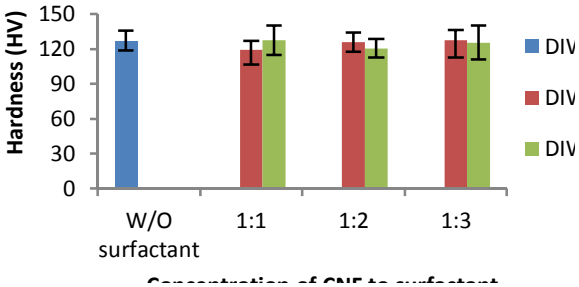

Figure 1 Comparison of surface hardness when using different types of dielectric fluid.

3.2 *Recast layer*

The variations of recast layer thickness with different concentration of GA and PVP surfactants added in dielectric fluid were illustrates in Figure 2. The result shows that the recast layer thickness produced when using dielectric fluid without surfactant was 13.03µm. Meanwhile, PVP surfactant illustrates lower recast layer thickness for all concentrations if compared with the dielectric fluid with GA surfactant and dielectric fluid without surfactant. This means that PVP surfactant gave better result because the lower thickness of recast layer will give less effect on the topography of machined surfaces. It can be seen that recast layer thickness is significantly influenced by the types of surfactant. Besides that, GA surfactant with 1:2 (concentration of CNF to surfactant) has produced highest recast layer thickness in turn resulted in high surface hardness. However, when using 1:1 concentration of CNF to GA surfactant in dielectric fluid, the recast layer produced was 12.57µm which is lower than the one without surfactant. It can be concluded that the concentration of CNF and surfactant also give effects on the characteristics of the recast layer. This recast layer is the result of the re-solidification of the melted material which did not sweep away from the stainless steel surface by the dielectric fluid during the EDM process.

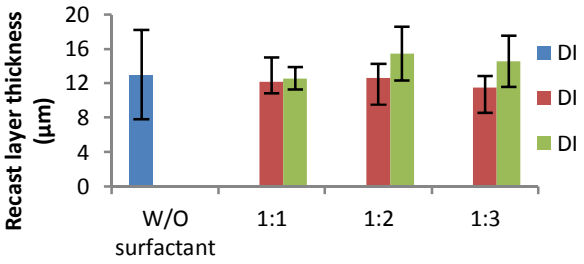

Figure 2 Variations of recast layer thickness with different types of dielectric fluid.

4. CONCLUSION

In this study, the effect of different types of surfactant on the surface integrity of AISI 304 stainless steel using EDM was investigated. The results show that by adding surfactants in dielectric fluid, the hardness of machined surfaces was insignificant. Meanwhile, by adding PVP surfactant in dielectric fluid, the recast layer thickness decreased significantly compared to the one using dielectric fluid with GA surfactant and without surfactant.

ACKNOWLEDGEMENT

Authors are grateful to Universiti Teknikal Malaysia Melaka for the financial support under the grant number RACE/F3/TK4/FKP/F00300 for the accomplishment of this work.

REFERENCES

[1] P.R. Dewan, "Latest trends in electro discharge machining," *European J. Advances in Eng. & Tech.*, pp. 66 – 71, 2015.

[2] M. Kolli and A. Kumar, "Effect of dielectric fluid with surfactant and graphite powder on electrical discharge machining of titanium alloy using taguchi method," *Inter. J. Eng. Sci. Tech. 18*, pp. 524 – 535, 2015.

[3] P. Pecas, and E. Henriques, "Electrical discharge machining using simple and powder-mixed dielectric: The effect of the electrode area in the surface roughness and topography," *J. Mater. Process. Tech. 200*, pp. 250 – 258, 2008.

[4] P.J. Liew, J. Yan, and T. Kuriyagawa, "Carbon nanofiber assisted micro electro discharge machining of reaction-bonded silicon carbide," *J. Mater. Process. Tech. 213*, pp. 1076 – 1087, 2013.

[5] S. Kumar, R. Singh, T.P. Singh, and B.L. Sethi, "Surface modification by electrical discharge machining: A review," *J. Mater. Process. Tech. 209*, pp. 3675 – 3687, 2009.

[6] K.L. Wu, B.H. Yan, J.W. Lee, and C.G. Ding, "Study on the characteristics of electrical discharge machining using dielectric with surfactant," *J. Mater. Process. Tech. 209*, pp. 3783 – 3789, 2009.

Proceedings of Innovative Research and Industrial Dialogue'16, pp. 163-164 (May 2017)

Effect of current density on the properties of nickel-fly ash composite coating deposited on aluminium alloy 7075 substrate

M.K. Ahmad, I.S. Othman*, M.Z. Zainal Abidin, M.F. Haikal Ali

Carbon Research Technology Research Group, Advanced Manufacturing Centre, Faculty of Manufacturing Engineering, Universiti Teknikal Malaysia Melaka, Hang Tuah Jaya, 76100 Durian Tunggal, Melaka, Malaysia

*Corresponding e-mail: intan_sharhida@utem.edu.my

Keywords: Fly Ash, Ni-FA Composite Coating, AA7075

ABSTRACT – The nickel- fly ash (Ni-FA) composite coatings were deposited on zincated aluminium alloy 7075 substrate by using electrodeposition technique. The electrodeposition process was carried out for 1 hour at 40ºC under the current density of 1, 3, 6, 9 and 12 A/dm^2 in a modified nickel Watt's bath containing FA particles. The produced composite coatings were characterized and tested using scanning electron microscopy, microhardness and wear test. As current density increase, the colonies like morphology of the Ni-FA composite coating become larger and denser. The co-deposited of FA particles also lead to significant increase in hardness and wear resistance.

1. INTRODUCTION

Aluminium alloy 7075 (AA7075) which have high strength-to-density ratio are widely used in marine, automotive and aerospace industry. However, according to Bocking and Reynolds [1] and Visser [2], it has low hardness and wears resistance, as well as susceptible to surface degradation when exposed to elevated temperatures. Therefore, nickel composite coating is introduced to AA7075 to improve its properties. Based on Nguyen et al. [3] and Boonyongmaneerat et al. [4], the composite coatings produced from the electrodeposition process have excellent surface properties, such as high hardness, high abrasion, high corrosion resistance and low friction coefficient.

In this study, the fly ash (FA) particles are added to the Ni watts bath solution. The FA can be employed as inexpensive strengthening particles which can increase wear resistance and enhanced micro-hardness and have low density [5]. According to Rashidi and Amadeh [6], current density plays an important role to the grain size of the electrodeposited coatings. Grain size decrease due to higher nucleation rate associated with higher current density [7].

Hence, the effect of current density on Ni composite coating deposited on AA7075 substrate are still less known. Thus, the present work is aimed to investigate the influence of various current densities for electrodeposition of Ni- FA composite coating on AA7075 substrate.

2. METHODOLOGY

The aluminium alloy 7075 (AA7075) substrate with dimension 40 mm x 30 mm x 3 mm were grind using silicon carbide papers of 180, 600, 800 and 1200 grit. The substrates were first cleaned with acetone, and then followed by immersion in 10 wt. % of sodium hydroxide (NaOH) solution for 10 seconds and immersion in 50 vol. % of nitric acid (HNO_3) for 20 seconds. The zincating process was carried out by dipping the pre- cleaned substrate vertically in a small glass beaker containing a zincating solution for 5 minutes at room temperature.

The chemical composition and operating condition for electrodeposition of Nickel-Fly ash (Ni-FA) composite coating on AA7075 substrate were summarized in Table 1. The surface morphology of Ni-FA composite coatings were examined by using SEM. The sliding wear properties of the Ni-FA composite coating were evaluated using pin-on-disk apparatus. The micro-hardness testing was performed using micro Vickers hardness tester.

Table 1: Composition of modified nickel Watt's bath solution and its operating condition

Composition	Concentration (g/L)
Nickel sulphate hexahydrate	200
Nickel chloride	20
Boric Acid	30
Sodium citrate	30
Operating condition	
Temperature (°C)	40
Deposition time (min)	60
Current density (A/dm^2)	1, 3, 6, 9, 12
Composition of FA (g/L)	25

3. RESULTS AND DISCUSSION

The SEM micro-graph images (Figure 1) showing a colony like morphology, which consists of lot of nickel grain crystal which having various sizes. At current density 1 to 6 A/dm^2, the micro-graph images show the more compact structure. However, as current density increase to 9 and 12 A/dm^2, the structures start to become larger and less compact. According to Rashidi and Amadeh [6], the SEM images points that the crystal shape convert from small to large crystal shape, this is because the increasing current density resulted the shape of crystal become larger and denser.

As current density increase, the micro-hardness of the Ni-FA composite coating also increased (Figure 2). Based on Yundong et al. [8], the increase in hardness value due to the grain refinement effect by increased in current density. According to C.N. Panagopoulos et al.

[9], the presence of hard oxides such as SiO_2 and Al_2O_3 contained in the fly ash helps in particle strengthening which lead to increase in hardness value of the coating.

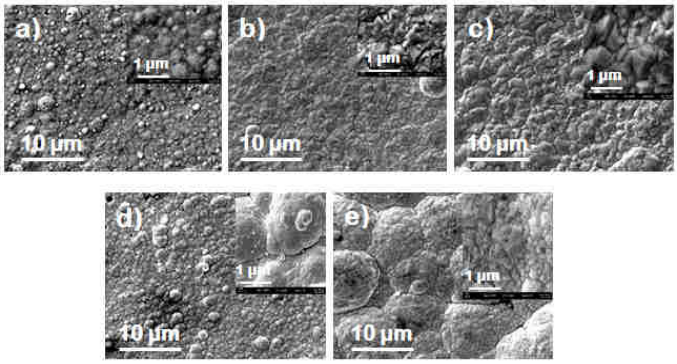

Figure 1: SEM micrographs of Ni-FA composite coatings produced at various current densities: (a) 1A/dm², (b) 3A/dm², (c) 6A/dm², (d) 9A/dm² and (e) 12A/dm².

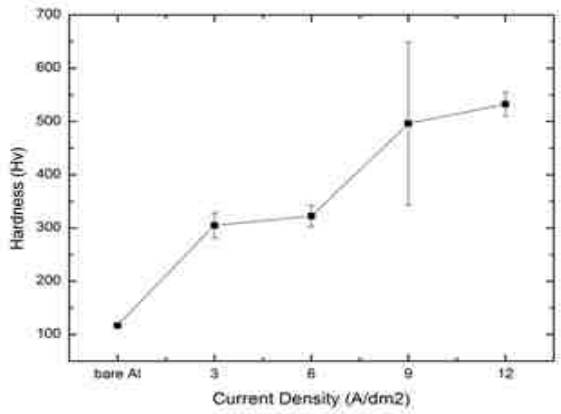

Figure 2: Microhardness for Ni-FA composite coatings produced at variouscurrent density of 3, 6, 9, 12 A/dm^2

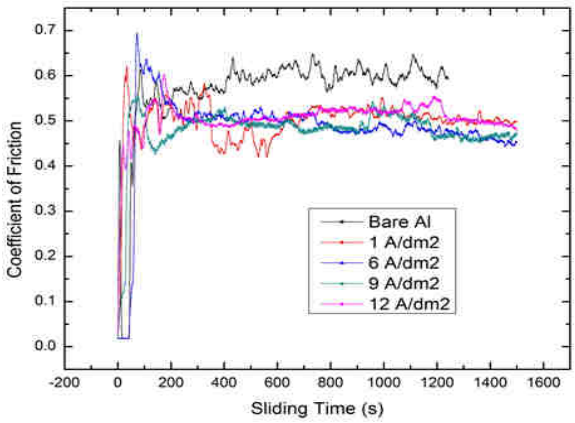

Figure 3: Coefficient of friction between bare Al with 1 A/dm^2, 6 A/dm^2, 9 A/dm^2 and 12 A/dm^2 of Ni-FA composite coating

From the result, it shows that, as current density increase there is not much difference between the coefficient of friction (COF). Compare to bare Al, the Ni-FA composite coatings exhibit better wear resistance. This may due to the tribological oxide layer can act as a lubricant layer between contact surfaces and decreases the friction coefficient based on Baghal et al. [10] previous works.

4. CONCLUSIONS

From the experimental investigation given, the influence of various current densities in the Ni-FA composite coating has improved the properties as the current densities increased from 1 A/dm^2 to 12 A/dm^2. In the following are the conclusions that can be made:

- As current density increased, the colonies like morphology become larger and denser.
- The coefficient of friction of Ni-FA composite coatings exhibit lower value when compare to bare AA7075. Thus, it indicates that Ni-FA composite coating have better wear resistance.
- Micro-hardness of Ni-FA composite coatings show that as current density increases, the hardness value also increases.

REFERENCES

[1] Bocking, C. and A. Reynolds, *Mechanism of adhesion failure of anodized coatings on 7075 aluminium alloy*. Transactions of the Institute of Metal Finishing, 2011. 89 (6): p. 298-302.

[2] Visser, P., *Novel totally chrome free corrosion inhibiting coating technology for protection of aluminium alloys*. Transactions of the Institute of Metal Finishing, 2011. 89 (6): p. 291-294.

[3] Nguyen, V. H., Anh, T., Ngo, T., Pham, H. H., & Nguyen, N. P. (2013). Nickel composite plating with fly ash as inert particle. Transactions of Nonferrous Metals Society of China, 23(8), 2348–2353.

[4] Boonyongmaneerat, Y., Saengkiettiyut, K., Saenapitak, S., & Sangsuk, S. (2009). Surface & Coatings Technology Effects of WC addition on structure and hardness of electrodeposited Ni – W. *Surface & Coatings Technology*, *203*(23), 3590–3594.

[5] Paper, C., & Oguocha, I. (2007). Effect of fly ash reinforcement on the corrosion behaviour of cast Al-Mg alloy A535 in 3.5 wt.% NaC1 solution, (May).

[7] Rashidi, A. and Amadeh, A. (2008). The effect of current density on the grain size of electrodeposited nanocrystalline nickel coatings. Surface and Coatings Technology, 202(16), pp.37 7 2-37 7 6.

[8] Yundong , Hui J, Weihua H, Hui T. (2008). Effects of peak current density on the mechanical properties of nanocrystalline Ni–Co alloys produced by pulse electrodeposition. Applied surface science,254(208).

[9] Panagopoulos, C. N., Georgiou, E. P., Tsopani, A., & Piperi, L. (2011). Applied Surface Science Composite Ni – Co – fly ash coatings on 5083 aluminium alloy. Applied Surface Science, 257(11), 4769–4773.

[10] Baghal, S. M. L., Sohi, M. H., & Amadeh, A. (2012). Surface & Coatings Technology A functionally gradient nano-Ni – Co / SiC composite coating on aluminum and its tribological properties. Surface & Coatings Technology, 206(19-20), 4032–4039.

Proceedings of Innovative Research and Industrial Dialogue'16, pp. 165-166 (May 2017)

Swell properties and dynamic mechanical behavior of natural rubber vulcanizates modified by tapioca starch

M. Mazliah[1], N. Mohamad[1*], H.E.Ab Maulod[2], I.S.Othman[1], P.J.Liew[1], M.A.Azam[1], M.E.A. Manaf[1], M. Zaimi[1], Q. Ahsan[1], S. Ismail[1], A.R.Jeefferie[1], A.Muchtar[3]

[1)] Carbon Research Technology, Advanced Manufacturing Centre, Faculty of Manufacturing Engineering, Universiti Teknikal Malaysia Melaka, Hang Tuah Jaya, 76100 Durian Tunggal, Melaka, Malaysia

[2)] Carbon Research Technology, Advanced Manufacturing Centre, Faculty of Engineering Technology, Universiti Teknikal Malaysia Melaka, Hang Tuah Jaya, 76100 Durian Tunggal, Melaka, Malaysia

[3)] Department of Mechanical & Materials Engineering, Faculty of Engineering, Universiti Kebangsaaan Malaysia, 43600 Bangi, Selangor, Malaysia

[*]Corresponding e-mail: noraiham@utem.edu.my

Keywords: Natural Rubber; swelling; tapioca starch

ABSTRACT – The effect of tapioca starch (TS) on swell properties and dynamic mechanical properties of natural rubber vulcanizates modified by tapioca starch was investigated. The samples were prepared by melt compounding via a Haake internal mixer. The tapioca starch was varied from 0, 5, 10, 20, 40, and 60 phr in the formulation. The crosslink density enhanced with the increase of tapioca starch and represented by the decrement in swelling percentage. In contrast, glass transition temperatures (T_g) of the NR vulcanizates decreased to -53.80°C as starch content increased from 0 to 60 phr. The improvement of damping properties was shown by the decreased in tan delta (δ).

1. INTRODUCTION

Recently, the use of fillers from organic nature has been the object of interest due to their low cost and light weight. Aside of being environmentally friendly in nature the produced composites exhibit enhancement in the mechanical properties [1-2]. Several cellulosic materials such as nut shells, bamboo, ground wood waste, cereal straw and white rice husk have been used as fillers for plastics [3] and elastomers [4].

Starch is one biopolymer substances most widely found in nature and mostly consists of amylose and amylopectin. There are several works of reinforcing elastomers with tapioca starch [4-6], but only a few addressed the physical and thermal properties of the unfilled vulcanizates. Thus, the aim of this study is to study the effects of starch content on the swelling and dynamic mechanical behaviour of NR vulcanizates. This study is part of our research work to produce biodegradable natural rubber based composites.

2. RESEARCH METHODOLOGY

2.1 Materials

Natural rubber (NR) with commercial trade name of 'SMR20' was purchased from Felda Global Ventures Holdings Bhd (FGV). Natural rubber was masticated with two-roll mill for about 10 min at 30 °C prior to compounding. TS was used as compound modifier and purchased from Polyscientific Enterprise Sdn Bhd. Other compounding ingredients such as sulfur, zinc oxide, stearic acid, were purchased from Systerm Classic Chemical Sdn. Bhd. Tetramethylthiuram disulfide (Perkacit-TMTD) was purchased from Aldrich Chemistry, while n-(1,3-dimenthyl)-n'-phenyl-p-phenylenediamine (6PPD) was supplied by Flexys America, USA. All compounding chemicals were used as received without further purification steps.

2.2 Sample preparation

The NR was compounded using a Haake internal mixer working at 60°C and a rotor speed of 60 rpm for 7 minutes per ASTM D-3192. The formulation recipes used in the present study are shown in Table 1. Then, the compounds were subsequently molded at 160°C and 150 kgf using a hot press model GT7014-A from GoTech.

Table 1 Formulation recipe used in the preparation of the composites

Materials	Compound (phr)[a]
Natural rubber	100
Zinc oxide	5.0
Stearic acid	2.0
TMTD[b]	1.0
6PPD[c]	1.0
Sulfur	2.5
Tapioca starch	5 / 10/ 20 / 40 / 60

[a] Parts per hundred

[b] Tetramethylthiuram disulfide

[c](1,3-dimethylbutyl)-N'-phenyl-p-phenylenediamine

2.3 Swelling measurement and crosslink density

Swelling measurement tests of the NR vulcanizates at different starch loading were performed in accordance with ISO 1817. The vulcanizates were immersed in toluene for 24 hours before the toluene uptake was calculated from the weight difference [7].

2.4 Dynamic mechanical analysis (DMA)

Thermal analysis was performed using a TA Instruments DMA-7 apparatus under a nitrogen purge at a frequency of 5 Hz and a heating rate of 2°C min-1.

3. RESULTS AND DISCUSSION

3.1 Swelling and crosslink density

The interaction between percentage of swelling and the crosslink density for NR vulcanizates is depicted in Figure 1. High crosslink density of the chain networks reduced the percentage of swelling [6, 8]. This is in good agreement with the increasing M_H-M_L value observed in our previous work [2]. These criteria obstruct the penetration of solvents since swelling only takes place when the osmotic pressure exerted on the rubber blend by the solvent is stronger than the cohesive forces between the rubber molecules [8]. Hence, the osmotic pressure exerted by the toluene reduces as the tapioca starch increases in the NR vulcanizates.

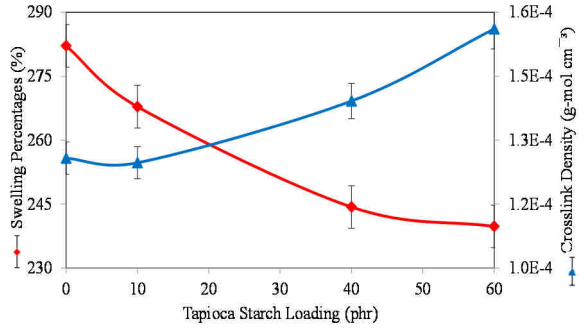

Figure 1 Correlation plot of NR vulcanizate's cure characteristics with tapioca starch loading

3.2 Dynamic mechanical behavior

Figure 2 shows the changes of T_g for NR vulcanizates at the range of -53.10 °C to -53.80 °C as starch content increased from 0 to 60 phr.

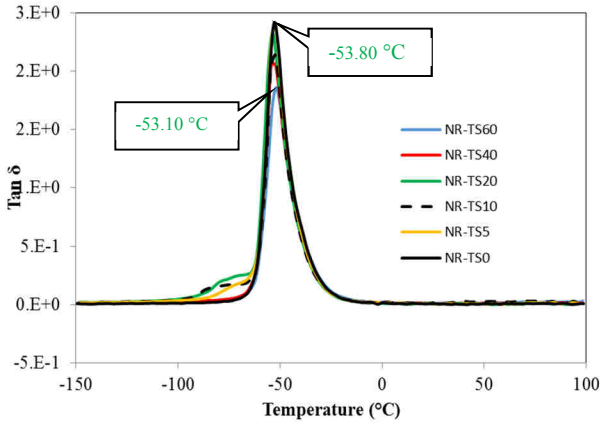

Figure 2 The Tan δ of the NR vulcanizates at 5.0 Hz versus temperature

The presence of tapioca starch hinders the relaxation process hence, lowering the T_g by enhancing the chain mobility of the NR. It can be explained by the decrease of curing rate with the increasing TS loading [2]. Furthermore, the presence of nearly single and sharp peaks of the tan δ indicates degree of miscibility between TS and NR [9] which improved at TS loading higher than 20 phr. The reduction of Tan δ depicts improvement of elastic response with TS loading.

4. CONCLUSIONS

The presence of tapioca starch (TS) in NR promotes the crosslink density but inferior to composite's damping properties which reflected by the decrement of Tan δ. It assists the molecular motion of rubber chains and facilitate the resilience of the composites under loading.

ACKNOWLEDGEMENT

The authors acknowledge UTeM for funding under the project number of PJP/2016/FKP/HI6/S01484.

REFERENCES

[1] J.L. Mo, Z.G. Wang, G.X. Chen, T.M. Shao, M.H. Zhu et al., "The effect of groove-textured surface on friction and wear and friction-induced vibration and noise," *Wear*, vol. 301, no. 1–2, pp. 671–681, 2013.

[2] M. Mazliah, N. Noraiham, A.R. Jeefferie, and H.E. Ab Maulod, "Cure characteristics and tensile properties of natural rubber vulcanizates modified by tapioca starch," in *Proc Mechanical Engineering Research Day 2016*, 2016, pp. 163-164.

[3] C. Nakason, A. Kaesman, S. Homsin and S. Kiatkamjornwong, "Rheological and Curing Behavior of Reactive Blending I. Maleated Natural Rubber-Cassava Starch," *J Polymer Science*, vol. 81, pp. 2803-2813, 2001.

[4] A.W.M. Kahar and H. Ismail, "High-density polyethylene/natural rubber blends filled with thermoplastic tapioca starch: Physical and isothermal crystallization kinetics study," *J Vinyl and Additive Technology*, 2014.

[5] A.W.M. Kahar, H. Ismail, and N.K. Othman, "Compatibilization effects of PE-g-MA on mechanical, thermal and swelling properties of high density polyethylene/ natural rubber/ thermoplastic tapioca starch blends," *Polymer-Plastics Technology and Engineering*, vol. 51, pp. 298-303, 2012.

[6] Y.H. Lum, A. Shaaban, N.M.M. Mitan, M.F. Dimin, N.Mohamad et al., "Characterization of urea encapsulated by biodegradable starch-PVA-glycerol," *J Polymers and the Environment*, vol. 21, no. 4, pp. 1083-1087, 2013.

[7] A.R., Jeefferie, Haji Ahmad, S., Ratnam, C.T., M.A. Mahamood, N. Mohamad, "Effects of PEI adsorption on graphene nanoplatelets to the properties of NR/EPDM rubber blend nanocomposites," *J Mater Sci*, vol. 50, pp. 6365 – 6381, 2015.

[8] B. B. Konar, S. K. Roy, and T. K. Pariya, "Study on the Effect of Nano and Active Particles of Alumina on Natural Rubber-Alumina Composites in the Presence of ENR as Compatibilizer," *J Macromolecular Science Part A-Pure and Applied Chemistry*, vol. 47(5), pp. 416–422, 2010.

[9] C. Sirisinha, P. Saeoui, and J. Guaysomboon, "Oil and thermal aging resistance in compatibilized and thermally stabilized chlorinated PE/NR blends," *Polymer*, vol. 45(14), pp. 4909–4916, 2004.

Proceedings of Innovative Research and Industrial Dialogue'16, pp. 167-168 (May 2017)

Water resistant composite sheet from durian shell waste using polyethylene as hydrophobic agent through disintegration method

R.F. Munawar*, A.B. Afraha, W.N.F.W.A. Shani, K.T. Lau, I.S. Othman, M.S.M. Suan, M.F. Dimin, P.J. Liew

Carbon Research Technology Research Group, Advanced Manufacturing Centre, Faculty of Manufacturing Engineering, Universiti Teknikal Malaysia Melaka, Hang Tuah Jaya, 76100 Durian Tunggal, Melaka, Malaysia

*Corresponding e-mail: rosefarahiyan@utem.edu.my

Keywords: Hydrophobic; polyethylene; durian shell

ABSTRACT – Easily being absorbed by moist or water is one of the main problems in existing composite sheet for which a special treatment is needed to limit its hygroscopicity and maximize its application. Biomass-derived materials such as durian shell, bamboo, sugarcane bagasse and kenaf are the perfect candidate to produce composite sheet in replacing wood. Due to this issue, alternative solution has been developed where the waste from natural resources is used. Furthermore, using agro-based materials can reduce the cost of producing composite sheet while giving added value to the waste. Therefore, this research investigates the effect of blended polyethylene (PE) to durian shell composite sheet surface through disintegration technique. Two important analyses have been conducted which are surface morphology analysis and water contact angle analysis. The addition of polyethylene (PE) has escalated the water resistance of the composite sheet with a water contact angle of 102.00° which exceed 90°.

1. INTRODUCTION

Hydrophobic material is defined as material and coating that obtained water contact angle larger than 90°. It can be achieved by increasing the roughness of the surface and decreasing the surface energy coating [1]. Hydrophobic and superhydrophobic materials own special characteristics such as water proof, self-cleaning and anticorrosion [2]. These unique features can be applied as packaging container, self-cleaning glass, non-wetting clothes, printing paper and business cards.

Durian shell is a new material selected in composite sheet making due to its hard in shell texture. This property will benefit in producing stronger composite sheet in terms of its mechanical properties. In order to avoid using wood that involves cost such as keno and others, wastes such as paddy straw and sugar cane bagasse can be utilized. Nowadays, modern technology enables us to explore beyond the ordinary and gives us the opportunity to turn durian shell wastes into money-making valuable product.

However, natural fiber has high water content and easily absorb moist from surrounding due to its hygroscopy property. This situation has depressingly affected the quality of the composite sheet. Thus, proper treatments ought to be applied, for various and long-term usage of composite sheet products.

Therefore, in this study, a water resistant composite sheet surface was prepared by adding polyethylene (PE) through disintegration technique. The addition of blended PE is believed would overcome the issue of hygroscopicity and gives water repellence properties to the composite sheet surface. The method selected was modified from Nurul Izzati et al. [3] and chosen based on the features of simplicity, cost efficiency and non-toxicity. PE is used widely as a coating agent against corrosion for steel pipe [4] and cage fishing net [5].

2. METHODOLOGY

2.1 Sample preparation

Durian shells (Durio zibethinus Murray) were obtained from local stalls in Melaka. They were chipped into smaller size which was about 3 cm in length and 0.3 cm in thickness after being washed with dionized water to get rid of unwanted constituents on their surface. Next, the durian shell chips were dried at 50 °C for 24 hours in drying oven to remove moisture.

2.2 Pulping

Pulping was carried out to remove lignin from cellulose via soda pulping method. The process was performed by using rotary digester machine. About 300 g of oven-dried of durian shell chips were pulped. The process was carried out with 17 % active alkali, at 170 °C for 2 hours. The ratio of durian shell chips to cooking liquor is 1:7.

2.3 Preparation of hydrophobic durian shell composite sheet

Durian shell pulp was well disintegrated and blended with low branched (LB) polyethylene in a mechanical disintegrator at 10,000 rpm for 25 min. The LB has 1.35 to 1.80 mm fibre length. It is white in colour, powder form, with a melting point of 135 °C. The ratio of durian shell pulp to PE was 7:3. The blended pulp mixtures were then being compressed using Paper Press machine with 16 cm of diameter in circular shape. The wet handsheets then were oven-dried for 30 min at 140 °C [3].

2.4 Characterization

Carl Zeiss of 1450VP model variable pressure scanning electron microscope (SEM) was used to observe the surface morphology of the samples while FECA contact-angle meter was used to measure the contact angle between the water and the surface of the

durian shell composite sheet. A total of five samples were measured for both analyses.

3. RESULTS AND DISCUSSION

PE is found as one of the strongest and lightest materials in the world that are suitable to be used in natural fiber. In this technique, the low density grade of PE is used because it is softer, good formability, more flexible, and able to melt at lower temperature compared to high density and linear low density grade of PE [3].

3.1 Surface morphology

PE acts as synthetic fiber that contributed to the hydrophobic properties. PE inhibited the ability of fluid either liquid or gas to penetrate easily into the surface structure of the composite sheet [3]. The surface morphology image of the durian shell composite sheet is shown in Figure 1. The figure shows the voids or pores among and between the durian shell fibres linkages. It also shows the melted area of the PE on the fibres surface and the pores. It is clearly observed that PE formed a layer of coating on the surface of the durian shell composite sheet. It is actually filled in the superficial pores, as shown in the figure. Though, there are still voids detected on the surface of the composite sheet. The PE was spread in the fibre linkages instead of covering the surface of the composite sheet. By using this disintegration technique, PE was present in between of the fibres in a different mechanism of immersion technique. The high content of PE has lessened the void volumes in the sample. This finding was supported by the research done by Heinrich [6] that PE is functioned as a heat sealable fiber that can melt and seal the voids within fibres.

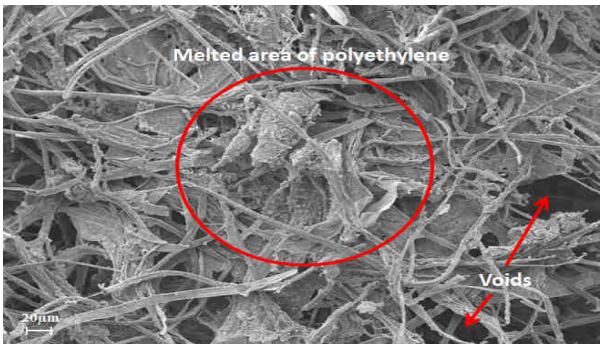

Figure 1 SEM micrograph of durian shell composite sheet surface

3.2 Water contact angle

Water contact angle is one of the important analyses in measuring hydrophobic properties of surface. Figure 2 shows the image of a water droplet on the surface of the durian shell composite sheet sample. The composite sheet was successfully achieved hydrophobic stage with a water contact angle of 102.00°. The hydrophobicity was attained from the production of crystalline properties from the PE.

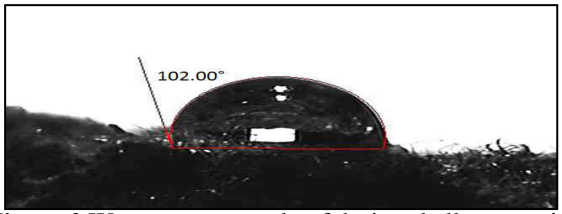

Figure 2 Water contact angle of durian shell composite sheet surface

4. CONCLUSIONS

A hydrophobic surface of durian shell composite sheet with a water contact angle 102.00° is successfully produced through disintegration technique with polyethylene (PE). This technique can be as one of other alternative techniques for fabricating water-resistant composite sheet. Besides, the additional of other hydrophobic agent to polyethylene may increase the stage of water repellency from hydrophobic to superhydrophobic.

ACKNOWLEDGEMENT

The authors are grateful to Universiti Teknikal Malaysia Melaka (UTeM) and Ministry of Higher Education, Malaysia for supporting this research under Fundamental Research Grant Scheme (FRGS): FRGS/2013/FKP/TK06/02/2/F00157. Also, a deepest gratitude expressed to The Faculty of Manufacturing Engineering and Carbon Research Technology Research Group of Universiti Teknikal Malaysia Melaka for providing the facilities.

REFERENCES

[1] A. Rawal, S. Sharma, V. Kumar, and H. Saraswat, "Designing superhydrophobic disordered arrays of fibers with hierarchical roughness and low-surface-energy," *Appl. Surf. Sci.*, vol. 389, pp. 469–476, 2016.

[2] S. Pan, N. Wang, D. Xiong, Y. Deng, and Y. Shi, "Fabrication of superhydrophobic coating via spraying method and its applications in anti-icing and anti-corrosion," *Appl. Surf. Sci.*, vol. 389, pp. 547–553, 2016.

[3] M. Z. Nurul Izzati, M. A. Ainun Zuriyati, A. Luqman Chuah, A. Hazwani Husna, H. Jalaluddin, and J. Mohammad, "Water Absorbency and Mechanical Properties of Kenaf Paper Blended via a Disintegration Technique," *BioResources*, vol. 8, no. 4, pp. 5570–5580, 2013.

[4] T. M. A. A. EL-Bagory, H. E. M. Sallam, and M. Y. A. Younan, "Effect of strain rate, thickness, welding on the J–R curve for polyethylene pipe materials," *Theor. Appl. Fract. Mech.*, vol. 74, pp. 164–180, 2014.

[5] P. M. Ashraf and L. Edwin, "Nano copper oxide incorporated polyethylene glycol hydrogel: An efficient antifouling coating for cage fishing net," *Int. Biodeterior. Biodegradation*, vol. 115, pp. 39–48, 2016.

[6] G. Heinrich, "Heat sealable tea bag paper and process of producing same," 1992.

Parameters and properties relationship of thin steel plate joint using low energy arc welding

S.D.Sabdin*, N.I.S.Hussein, M.K.Sued, M.N.Ayof

Faculty of Manufacturing Engineering, Universiti Teknikal Malaysia Melaka, Hang Tuah Jaya, 76100 Durian Tunggal, Melaka, Malaysia

*Corresponding e-mail: saifulkdh@yahoo.com

Keywords: Thin plate; Arc welding; steel; heat input

ABSTRACT – One of the reasons in the development of thin plate welding technology is to minimize the cost and weight of the welds. This research aims to establish the relationship between welding parameters and heat input responses. A thin plate is welded using the low energy arc welding (ColdArc) machine on the ASTM A36 mild steel specimen. Effects of welding parameters to the weld performance are evaluated. It was found that output responses is related to the heat source, deformation of welded joint and its physical properties.

1.0 INTRODUCTION

A new variation on conventional short-circuit arc welding introduces changes to the electric current. The course of the arc's voltage in the ColdArc welding method is identical to the traditional short-circuit arcs, with only principle difference occurring in the course of its electric current. During welding, temperature variations in welds and parent metals have important effects on material characteristics, residual stresses as well as on dimensional and shape accuracy of welded products. This is important for thin sheet metal products, where control over welding distortions or deformations is difficult.

Investigation on effects induced to the welded structures for various applications of ColdArc has been done. Novel welding processes with lower heat input, based on pulsed welding arc, may effectively be used for fabrication of sheet metal products, reducing the problems related to the MIG process. The ColdArc process is considered as a prospective welding process when narrow fabrication tolerances and product quality are the constraints. Improvement for the quality, flexibility and productivity of the welding performance and the process of automatization using welding robots is important. Available information about welding parameters of the ColdArc process is scanty, yet essential for programming welding robots and creating welding procedure specifications (WPS).

2.0 METHODOLOGY

The experiments were conducted according to the information obtained from literature [1,2] using the welding parameters given in [3]. The robot welding used in this study was KUKA type KRC4 with the system is equipped EWM ColdArc power source. One specimen was used in welding of three welds with different welding parameters.

Welding was conducted on ASTM A36 mild steel. The material of 1.0 mm thickness was welded on the lap joint using a solid welding wire of diameter 1.0 mm grades ER70S-6 mild steel.

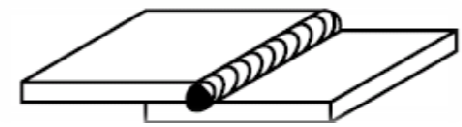

Figure 1 Lap joint

2.1 Heat Input

Heat input (Q) is a relative measure of the energy transferred per unit length of weld. It is an important characteristic because, like preheat and interpass temperature, it influences the cooling rate, which may affect the mechanical properties and metallurgical structure of the weld and the HAZ [4] .

$$Q = V \times I \times \frac{60}{v} \quad \text{kJ/mm} \qquad (1)$$

3.0 RESULTS AND DISCUSSION

Table 1 outlines the preliminary experimental result. Visual examination showed that unequal curvature and angle of the welding joints occurred. According to ISO 5817 of the standard for welding quality, welded joints can be classified according to uniform and regular joint.Figure 2 shows the results. In some specimens (Figure 2 (a) – (e)) partial penetration were observed. Lap joints welded with the same welding feed rate and higher welding speed resulted in surfaces pores.

Table 1 Preliminary experimental result

No	Parameter	No. of Sample				
		1	**2**	**3**	**4**	**5**
1	Welding speed (m/min)	0.4	0.6	0.6	0.6	0.6
2	Ampere(A)	70	70	70	77	78
3	Voltage (v)	18.5	18.5	19	17	17
4	Wire speed (m/min)	2.5	2.5	2.5	2.5	2.5
5	Pre flow time (s)	0.15	0.15	0.1	0.1	0.1
6.	Post flow time (s)	0.15	0.15	0.1	0.1	0.1
Visual (result)		x	x	√	√	x

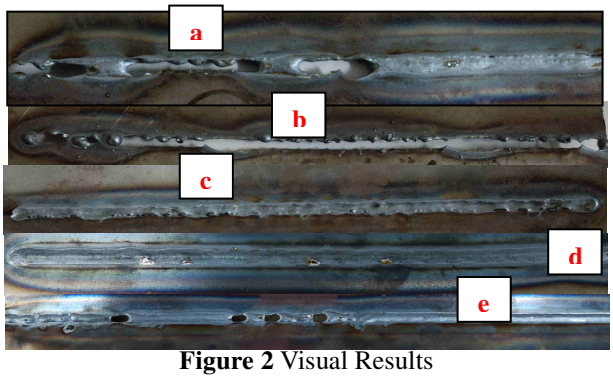

Figure 2 Visual Results

Figure 3 and 4 shows the relationship between speed and heat input and current and voltage, respectively. Heat input directly influences the distortions and deformations of welded parts and in case of thin sheet metal the optimal heat input is essential to guarantee the joint penetration with minimum heat input. Welding the mild steel with thickness of 0.5–1 mm, the heat input was in the range of 0.130–0.133 kJ/mm. For mild steel, further studies are to be conducted to determine the heat input parameters. The results obtained in this study correlate with the results obtained in [5], where the ColdArc technology was adopted for welding the similar metals. Excessive concavity was noted, also it depends on the welding speed and current. The ColdArc process proves to be suitable for welding thin sheet metal with- out spatters. It is essential to determine the right welding speed (speed range) to guarantee low porosity and to minimize distortions in the product. Using the above mentioned welding method and welding speed in the 0.6 m/min for welding mild steel proved to be the most appropriate. Further increase of the welding speed will cause concavity of the welded joint. This is the actual limit for further increase of productivity by increasing welding speed.

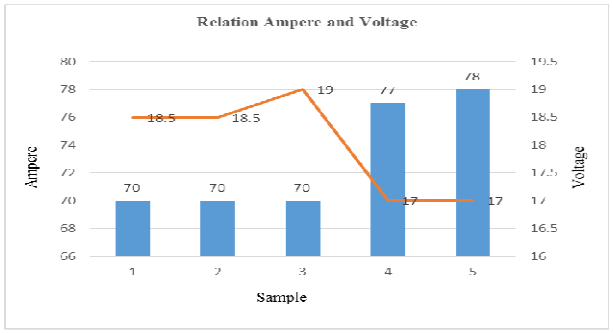

Figure 3 Ampere and voltage relationship

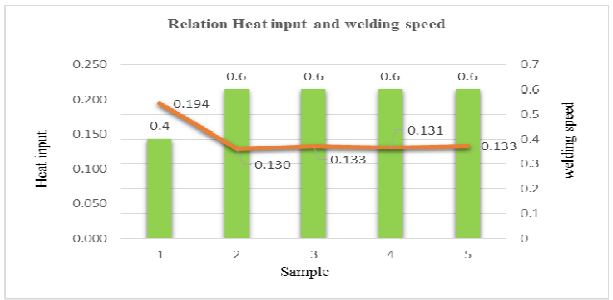

Figure 4 Welding speed and heat input relationship

Increasing the pre-flow and post-flow time robot welding to 0.15s can cause holes due to 0.1s greater weld bead. The low-energy welding methods allow the formation of lap joints of mild steel of 1mm thick characterized as high aesthetics, good mechanical and plastic properties. Achieving high quality of welded joints requires precise selection of welding parameters. Due to the very narrow window of suitable parameters, it is advisable to create a trial joint for a particular material before the actual welding begins, in order to validate the parameter settings and welding conditions.

4.0 CONCLUSIONS

Output responses are related to heat source, deformation of welded joint, thermal and physical properties. The study shown that these methods successfully applied to welding ASTM A36 mild steel of 1 mm thickness. Worth noting these methods allow creating lap joints of thin sheets, even with 1mm thickness, which was impossible using traditional welding tools with consumable electrodes in gas shielding, and MIG welding of such materials.

ACKNOWLEDGEMENT

The authors would like to thank the Faculty of Manufacturing Engineering, Universiti Teknikal Malaysia Melaka (UTeM) and Advanced Technology Training Center (ADTEC) Batu Pahat for education and technical supports.

REFERENCES

[1] P. Taylor and M. De Dompablo, “New solutions in coldArc and forceArc welding technology,” *Weld. Int.*, vol. 27, no. December 2014, pp. 37–41, 2013.

[2] P. Kah and J. Martikainen, “Current Trends In welding Processes And Materials : Improve In effectiveness,” *Rev. Adv. Mater. Sci.*, vol. 30, pp. 189–200, 2012.

[3] P. Miguel, S. Almeida, and N. Titanium, “Innovations in arc welding,” *5º Congr. Luso-Moçambicano Eng.*, no. April 2016, 2011.

[4] M. H. K. Chavan and D. M. S. Kadam, Mr. Gunwant D. Shelake, “Effect of heat input and speed of welding on Distortion,” *Int. J. Ind. Eng. Res. Dev.*, vol. 3, no. 2, pp. 42–50, 2012.

[5] R. Talalaev, R. Veinthal, A. Laansoo, and M. Sarkans, “Cold metal transfer (CMT) welding of thin sheet metal products,” *Est. J. Eng.*, pp. 243–250, 2012.

Proceedings of Innovative Research and Industrial Dialogue'16, pp. 171-172 (May 2017)

Morphological studies of porous beta-tricalcium phosphate scaffold using sacrificial template method

N.F. Ishak[1, 2], Z. Mustafa[1, 2*], R. Othman[1, 2,] N. Ahmad[3]

[1)] Faculty of Manufacturing Engineering, Universiti Teknikal Malaysia Melaka, Hang Tuah Jaya, 76100 Durian Tunggal, Melaka, Malaysia

[2)] Advanced Manufacturing Centre, Universiti Teknikal Malaysia Melaka, Hang Tuah Jaya, 76100 Durian Tunggal, Melaka, Malaysia

[3)] School of Materials Engineering and Mineral Resources, University Science Malaysia, 13400 Nibong Tebal, Penang

[*]Corresponding e-mail: zaleha@utem.edu.my

Keywords: Tricalcium Phosphate; Sintering; Particle size

ABSTRACT – The crystallization structure of porous TCP scaffold was investigated in this study. Beta-tricalcium phosphate scaffold was prepared using a sacrificial template method and thermally-treated at various sintering temperatures of 1400°C, 1450°C and 1500 °C. Morphological observation was conducted using a Scanning Electron Microscope (SEM) that revealed pore sizes in the range of 100 µm to 300 µm and the pores were interconnected. As the sintering temperature increased, less formation of voids were observed in the struts. Maximum morphological characteristics were observed at 1450°C, whilst beyond this temperature the presence of cracks was observed on the surface of the struts.

1. INTRODUCTION

Biomaterials have become progressively important in tissue engineering field to treat extensive bone defects, osteoporotic fractures, bone infections and bone tumours. Among others, bioactive calcium phosphate materials such as β-tricalcium phosphate (β-TCP) have been extensively utilized as bone implants in bone prostheses. Other than that, β-TCP is known to have substantial biological affinity and activity, and hence responds well to the physiological environments [1]. In the sintering process, the two different forms of TCP influence the morphological structure such as densification and grain growth [2]. Sintering at high temperatures will lead to the compaction and removal of pores from the material [3]. The main characteristics in the formation of porous scaffold for tissue engineering are the pore size (in the range of 100µm to 300µm) and good connectivity to allow proliferation of the cell growth as well as nutrient transportation can take place during application. The fabrication of porous ceramic scaffolds by using a template method is favourable due to their capability of creating uniform dispersion of ceramic powder inside the polymeric struts and at the same time producing high porosity structure [4]. In this study, the morphological characteristics of the β-TCP scaffold were investigated by optimising their sintering temperature.

2. METHODOLOGY

The β-TCP scaffolds were prepared via **a** sacrificial template method using polyurethane foam. Calcium phosphate ($Ca_3(PO_4)_2$) powder (Sigma Aldrich, United Kingdom) was mixed in 2% of polyvinyl alcohol aqueous solution (Merck, USA) at a powder to liquid ratio of 5/5 (wt/vol) to obtain a well-dispersed slurry. The 10 mm^3 scaffolds were produced by immersing the foam in the TCP slurry [4]. The dried slurry-impregnated foam specimens were subsequently subjected to three different firing protocols with maximum sintering temperatures of 1400 °C, 1450 °C and 1500 °C. Morphological properties were analyzed using a Scanning Electron Microscope SEM EVO 50 (Carl Zeiss, UK) at an accelerating voltage of 5kV. Particle size analysis of the β-TCP powder was performed using a particle size analyzer (Masterizer 2000, Malvern, UK).

3. RESULTS AND DISCUSSION

During the sintering process, the densification occurred due to pore elimination and this was achieved via the diffusion of matter through the grain boundaries between particles. Three different ceramic sponges used in this work exhibit a highly interconnected porous structure with open pores having an average size ranging from 150µm to 400µm. As shown in Figure 1(a), the β-TCP scaffold was not yet fully densified in comparison to Figures 1(b) and 1(c). As the sintering temperature increases, the struts surface appears to be smoother with less voids being formed. However, as the temperature increases to 1500°C, the formation of cracks starts to be observed (Figure 1c). This crack formation that occurred at the highest sintering temperature suggests that the stress increases as the temperature increases [6]. The β-TCP powder consists of a normal distribution of particle size with $d_{0.5}$ of 4.41µm. This contributes to a good compaction of the microstructure with less formation of voids during sintering as small particles fill-up the voids created by the large particles without expanding the overall system volume [7].

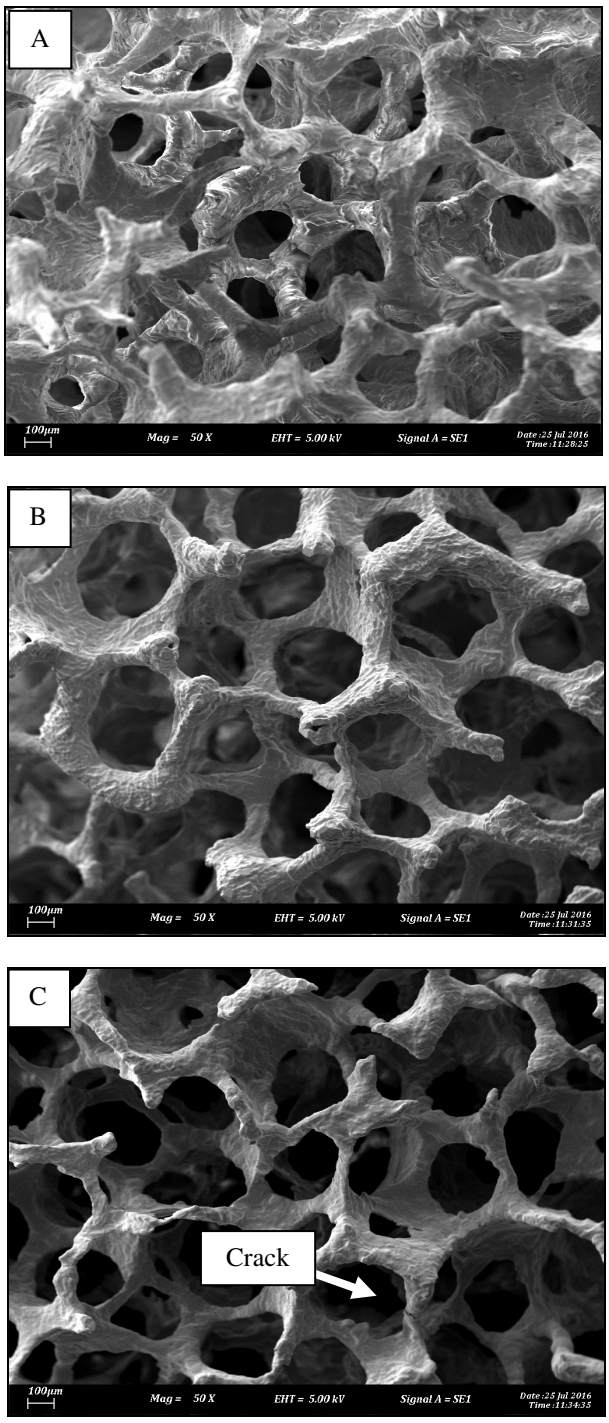

Figure 1. SEM images of porous TCP scaffolds at sintering temperature (a) 1400°C; (b) 1450°C; (c)1500°C

4. CONCLUSIONS

In conclusion, sacrificial template method has been successfully adopted to produce porous scaffold with pore size of 150µm to 400µm, which is within the desirable biomaterial requirement. As the sintering temperature increased, the surface of the scaffold struts revealed denser formation and less voids formed. At a maximum sintering temperature of 1500°C, crack starts to form on the strut surface. This suggests that the optimized sintering temperature to produce a porous scaffold is at 1450°C, and thus, can be further used for the next stage of the study.

ACKNOWLEDGEMENT

The authors are grateful to the Ministry of Education Malaysia for funding this research project under Research Acculturation Grant Scheme RAGS/1/2014/TK04/FKP/B00073 and Universiti Teknikal Malaysia Melaka (UTeM) for the use of laboratory facilities.

REFERENCES

[1] N., Kivrak and A.C. Taş, (1998). Synthesis of Calcium Hydroxyapatite□Tricalcium Phosphate (HA□TCP) Composite Bioceramic Powders and Their Sintering Behavior. *Journal of the American Ceramic Society*, 81(9), 2245-2252.

[2] Y.W., Gu, N.H., Loh, K.A., Khor, S.B. Tor and P. Cheang, (2002). Spark plasma sintering of hydroxyapatite powders. *Biomaterials,* 23(1), 37-43.

[3] D. Malina, K. Biernat and A. Sobczak-Kupiec (2013). Studies on sintering process of synthetic hydroxyapatite. *Acta Biochim Pol*, 60(4), 851-855.

[4] N.F. Ishak, Z. Mustafa, R. Othman, S.S.M. Fadzullah and A.M. Sahab, (2016). Effect of sintering on the physical properties of porous β-TCP scaffolds. *Proceedings of Mechanical Engineering Research Day,* 2016, 135-136.

[5] Padmanabhan, S. K., Gervaso, F., Carrozzo, M., Scalera, F., Sannino, A., & Licciulli, A. (2013). Wollastonite/hydroxyapatite scaffolds with improved mechanical, bioactive and biodegradable properties for bone tissue engineering. *Ceramics International,* 39(1), 619-627.

[6] M.Tillman, J.A. Yeomans and R. Dorey (2014). The effect of a constraint on the sintering and stress development in alumina thick films. *Ceramics International*, 40(7), 9715-9721.

[7] S. Schaefer, R. Detsch, F. Uhl, U. Deisinger and G. Ziegler (2014) How degradation of calcium phosphate bone substitute materials is influenced by phase composition and porosity. *Adv. Eng. Mater*. 13, 42–350.

Proceedings of Innovative Research and Industrial Dialogue'16, pp. 173-174 (May 2017)

A case study: workplace environment and activity potential towards slips and falls

S.A.S.S.Ali[1,*], K.S.R.Kamat[1]

[1)]Faculty of Manufacturing Engineering, Universiti Teknikal Malaysia Melaka, Hang Tuah Jaya, 76100 Durian Tunggal, Melaka, Malaysia

[*]Corresponding e-mail: aznee_78@yahoo.com

Keywords: slips and falls; floor; work activity

ABSTRACT – The workstation is riskiest area is equipped with the different types and size of tool, and material suite to the task. The kitchen is one of the riskiest workstation area to cause slips and falls incident. During the working period, the hazard comes from tools, material, floor, shoes, human and also task that can contribute to slips and falls accident. Because of such reason, this study needs to analyse the main factors that create hazards and potential to slips and falls. Forty training for final semester student were involved in Kitchen restaurant of Kristal Polytechnic Merlimau, Melaka. The trainee is divide by task. The training group experienced at least 1 year in kitchen workplace. Findings from this study can help to reduce the risk activity posture especially in the commercial kitchen.

1. INTRODUCTION

Slips and falls are an intriguing problem because can harm to anybody, anytime and everywhere. The workplace is a very hazardous area because employee spent 8 hours to 12 hours at their workplace. Although employees well train and provided with proper personal protective equipment suitable to their task, accidents still exist and sometimes increase yearly. Figure 1 shows the number of accident cases in Malaysia is about 47962 cases accident cause from Person falling from the same level are reported to SOCSO from year 2009 until 2014. The slips and falls accidents which had increased from year 2010 until year 2014 [1]. An increment of 5% is seen from the year 2010-2013. Cases on slips and falls keep on increasing from year to year.

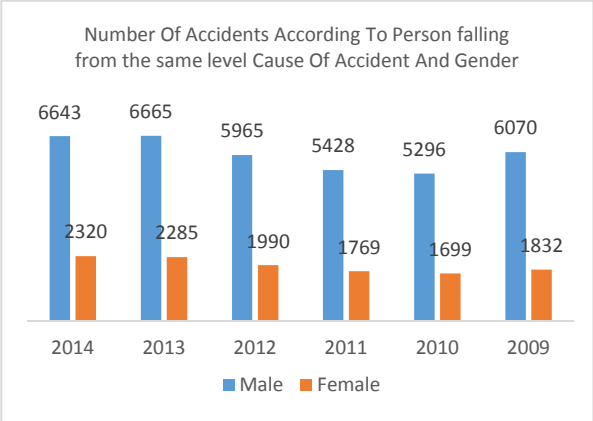

Figure 1 Number of Accidents According to Cause of Accident and Gender: Source (Annual report from SOCSO)

The workplace environment in the kitchen similarly contributes to slips and falls accident because of factors such as footwear, flooring, machine, lighting, contaminant like water and oil are nearly connected to slip and fall accident to employee. Figure 2 shows the number of accidents in Accommodation and Food Services Activities in Malaysia is about 12285 cases are reported to SOCSO from year 2009 until 2014 [1].

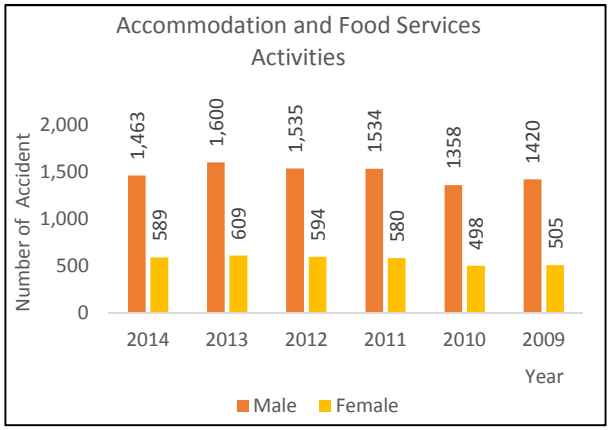

Figure 2 Number of Accidents According to Accommodation and Food Services Activities: Source (Annual report from SOCSO)

During working, active and longer pathways will produce the most slip and fall problems [2], [3] and [4]. At the kitchen workstation, position standing is used for the whole working day. Those utensil using in the kitchen such as cookware set, wok set, and pan set and also lunch or dinner plate is provided with different weight.

2. METHODOLOGY

The flow chart presented in Figure 3 for the process of this study. This project is starting with identifying the factor to contribute to slips and falls in the kitchen worplace. During the cooking process activity, forty trainer involves in four main departments such as delivery or service, cooking, dish clothing and washing utensils. A questionnaire survey was distributed amongst the trainer and observation will be recorded using a camera during kitchen activities.

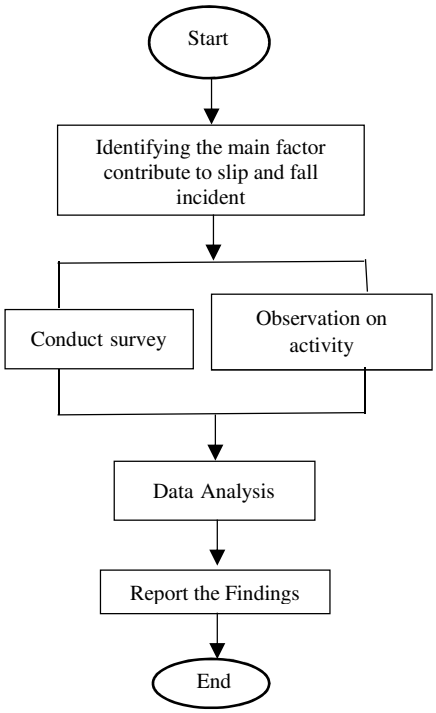

Figure 3 Process flow chart

3. RESULTS AND DISCUSSION

Figure 4, shows sign of slips and falls. From the response, the majority of the respondents who have seen the slips and falls signs are 82.5 % and 91.7 % of them know about slips and falls signs. And 17.5 % of the respondents have not seen the slips and falls signs similar to 8.3 % of respondents who did not know about slips and falls signs.

Figure 4 Slips and falls sign

Figure 5 shows the main factors that cause slips and falls. Flooring is contributing 28.6 % to main factor of slip and fall factor. Then footwear is the second lead to slip and fall with 18.8 %. The environment is third source that contributes to slip and fall by 13.3 %. Environment means the working area is unsuitable environment such as temperature and lighting level, there is some boxes or apparatus that are not in proper arrangement and so on. The fourth cause of slip and fall is cleaning with 12.9 %. Cleaning means there are some liquid on the walking area such as water, detergent or oily. People or human factor contributes 9.4 % of the cause to slip and falls. The sixth factor is obstacles which are 9.0 % of the respondent's vote for this factor. And 3.9 % of the respondent said that our health is responsible to cause slip and fall problems.

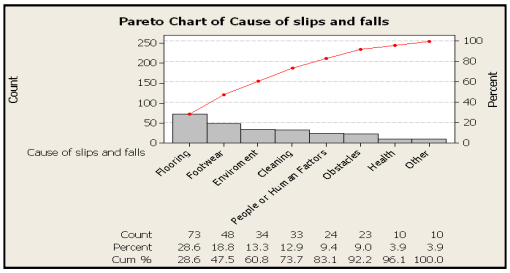

Figure 5 Slips and falls factors

Table 1 presents the summary data from questionnaire result. The working position can be categorized into 4 postures, which is 62% of the trainer use standing posture, 10% of trainer use bending posture, 20% of them use walking and less than 8% using walking as their working position. From the working posture, 68% of the trainers are feeling discomfort during the working activity. It is because most of the trainer is moving to surround the workstation from one station to another station. However, 80% of the trainer respondents that their working posture resulted in bad impact on safety and health personally.

Table 1 Questionnaire survey

Work position during working		Do you feel comfortable when in the workstation		During the period of work, have work station give a negative impact on the safety and health	
standing	62%	Yes	32%	Yes	80%
run	8%				
bending	10%	No	68%	No	20%
walking	20%				

4. CONCLUSIONS

Working environment is the main factors to cause a hazard to employees. Hence, daily activity in the working area will be easily to harm the employees and potential to develop unbalance problems, especially working with bad body posture for prolonged standing. Everybody has their own abilities and limitations, if the employee had an experienced with accident or health condition problem will easily contribute to balance problem. The combination of those factors will result in slip and fall accident. Finally, those victims face permanent serious injuries until fatalities. For future work will focus on the effect of working posture to human body towards slips and falls incident.

REFERENCES

[1] SOCSO Annual Report, Ministry of Human Resources, 2009-2014.

[2] Ralph Barnett, L. and A. Suzanne Glowiak, "Extreme Value Formulation of Human Slip: A Summary," *Triodyne Safety Brief*, vol. 27 no. 4, 2005.

[3] Ralph Barnett, L. and J. Peter Poczynok, "Slip and Fall Characterization of Floors," *Triodyne Safety Brief,* vol. 26 no. 2, 2004.

[4] Ralph Barnett, L., A. Suzanne Glowiak and J. Peter Poczynok, "Stochastic Theory of Human Slipping,"*Triodyne Safety Bulletin* vol 22 (4), 2003.

Proceedings of Innovative Research and Industrial Dialogue'16, pp. 175-176 (May 2017)

Hidden wastes of transportation between processes with respect to overall equipment effectiveness (OEE)

Y.S. Teoh [1,*], P. Puvanasvaran[1,*], T. Ito[2]

[1)] Faculty of Manufacturing Engineering, Universiti Teknikal Malaysia Melaka, Hang Tuah Jaya, 76100, Durian Tunggal, Melaka, Malaysia

[2)] Faculty and School of Engineering, The University of Tokushima
2-1 Minami Jousanjima-cho, Tokushima 770-8506, Japan

[*]ysteoh1987@hotmail.com; punesh@utem.edu.my

Keywords: Transportation; hidden wastes; Overall Equipment Effectiveness

ABSTRACT – Overall Equipment Effectiveness (OEE) measures single equipment with respect to time, speed and quality losses for monitoring purpose. However, interrupted material flow between processes which contributes lengthy lead time and waiting time are neglected in OEE. Transportation as the connector of processes is examined in term of its impact onto the processes that it connects with. Relations between transportation and the performance measures of destination processes could be established. Consequently, new mathematical model is proposed to quantify the relation and causes exist within transportation process. This ensures continuity of production system with minimal transportation, waiting time and shorter lead time.

1. INTRODUCTION

Overall Equipment Effectiveness (OEE) pursues equipment to run all the time at ideal speed and produce the amount not less than any other owners with same equipment with good quality. However, relations between processes is not established in OEE implementation to engender a sense of joint responsibility among all processes because the OEE focuses on single equipment only. This is harmful for the collaboration of operations and resources as there are many invisible issues and uncertainties within production system. The external issues include the unreliable downstream capacity, unpredictable variation of raw materials or work in progress in terms of delivery, quantity and quality, as well as fluctuation of market and customer demand [1]. They usually exist between processes.

Similarity of the outcomes from problematic production planning is the delay arrival of materials to planned customer processes. Therefore, comparison of demand with production amount is crucial from time to time. Company could adjust their lot sizes and safety stock level based on the demand and seasonal cycle of that particular product [2]. Transportation serves as the medium of connecting two consecutive processes should be monitored and improved to ensure efficiency of the material flow. Transportation could be measured and evaluated by Transportation Overall Vehicle Effectiveness (TOVE) from the perspective of vehicle performance and operating availability [3][4]. Operations research and mathematical modelling approaches could be applied in improving transportation performance. Villarreal et al. [5] demonstrated the usage of Transportation Overall Vehicles Effectiveness (TOVE), which is a modification on OEE focusing on routing operation. In short, mutual relations between machines and the ways they interact with each other should be emphasized to promote continuity of production with minimal transportation level. This could be achieved via quantification of transportation between processes with concept of OEE.

2. METHODOLOGY

The main focus of this study is to reveal hidden wastes especially on the transporting activities in terms of waiting time, its impact on utilization rate and lead time of material with respect to implementation of OEE. Site observation is carried out in a production line which consists of 5 processes so that its time data, equipment number and material flow have been collected. They are the basis in constructing simulation model which is then simulated for 30 replications and one month timeframe. Relation between operations of equipment with transportation is established based on the simulation result. A new mathematical model is proposed to monitor and minimize hidden wastes like waiting time, excessively running equipment due to ineffective transportation and long lead time of materials staying in production system.

3. RESULT AND DISCUSSION

Five consecutive processes studied in a selected company which are denominated as Process A, B, C through E in sequential order along with transportation operation between any two consecutives processes. 5 Forklift is shared within production system for the transporting purpose and 4 routes are required by forklift to transport a complete set of WIP from supplier process to customer process. The production system (Case A) is simulated to examine total waiting time and their utilization of resources at each process. Another scenario is simulated again (Case B) where the transportation time is halved as in Case A. Comparison is made between both cases as shown in Table 1:

Table 1 Waiting time and utilization rate at each process

Process	Waiting time (Hour)		Utilization (%)	
	Case A	Case B	Case A	Case B
A	849.47	623.36	66.53	63.75
B	340.87	235.09	51.08	49.24
C	0.09	0.86	6.60	6.31
D	684.02	412.58	74.69	72.05
E	3976.06	3817.99	68.87	69.19
Transp-ortation	160.68	29.16	38.03	18.28

From Table 1, improvement in transportation leads to slight reduction of equipment utilization and huge decline in waiting time. This is because equipment could process more materials at once due to readiness of materials and without over-processing in separate run. In actual, both cases produce 27 sets of product by the end of production system with variation of equipment utilization. Besides, ineffective transportation could contribute to lengthy lead time of material and this is invisible or hidden under implementation of OEE. This is proven by the simulation result as in Table 2 as below:

Table 2 Total time elapsed by entity at each process

Process	Total time per entity (Hour)	
	Case A	Case B
A	29.27	26.26
B	22.36	21.09
C	1.00	1.01
D	31.21	27.17
E	172.58	163.87
Transportation	9.82	3.93
Total Lead Time per Entity	266.24	243.33

Lead time data in Table 2 proves that effective transportation lowers the utilization at each process and less waiting time. Since the conventional OEE quantifies only the performance of single equipment, the impact of transportation on lead time of material in the production system has been neglected. It is necessary to quantify the hidden wastes by implementing OEE in transportation process with modifications on its three elements as shown below:

A_T = Total transport time/ Total service duration of forklift (1)

P_T = Total transported unit/ Total capacity of service vehicle (2)

Q_T = Total transported good unit/ amount required in next process (3)

It is more proper to evaluate availability with respect to the total service duration of forklift rather than total calendar time available which promotes maximization of transportation. This is because transportation is one of the lean wastes. The waiting time, loading and unloading time from forklift and breakdown of forklift are then excluded from the service duration to get the effective transportation time. On the other hand, performance ratio measures transported unit over the total size and capability of forklift whereas quality ratio measures the ability of forklift to fulfill the amount required by its destination process. Both of the performance and quality ratio promote One Time in Full (OTIF) without any excessive transportation to ensure continuity of production.

4. CONCLUSIONS

The paper has justified the hidden wastes in production system due to ineffective transportation between processes. It increases waiting time of all processes because of unavailability of materials to be processed on time. Besides that, frequent transportation leads to longer waiting time because the service vehicle is not always available immediately. Excessive utilization and long waiting time contribute to lengthy lead time of material in production system. Therefore, quantification of transportation using OEE concept has been proposed to encourage the transportation of up to capability of forklift in ensuring continuity of production. Requirement for transportation can be reduced via implementation of OEE and therefore reduce the waiting time for arrival of forklift and lead time of material.

ACKNOWLEDGEMENT

Authors are grateful to Universiti Teknikal Malaysia Melaka for the opportunity and Ministry of Higher Education of Malaysia for the financial support through Fundamental Research Grant Scheme numbered FRGS/1/2015/TK03/UTEM/02/5.

REFERENCES

[1] J. Lee, E. Lapira, B. Bagheri and H.A. Kao (2013). Recent advances and trends in predictive manufacturing systems in big data environment *Manufacturing Letters*, *1*(1), 38-41

[2] E. M. T. Colares, How to solve the trade-off between capacity utilization and service level

[3] D. Simons, R. Mason and B. Gardner (2004). Overall vehicle effectiveness. *International Journal of Logistics Research and Applications*, 7(2), 119-135

[4] B. Villarreal, (2012). The transportation value stream map (TVSM). European Journal of Industrial Engineering, 6(2), 216-233

[5] B. Villarreal, J.A. Garza-Reyes and V. Kumar, (2016). A lean thinking and simulation-based approach for the improvement of routing operations.*Industrial Management & Data Systems*, *116*(5), 903-925

Proceedings of Innovative Research and Industrial Dialogue'16, pp. 177-178 (May 2017)

Chassis design and analysis of narrow track vehicle

M.A. Abdullah[1,2,*], M.A.H. Mohd Najmi[1], M.H. Harun[1,2], F.R. Ramli[1,2] and S. Mat[1,2]

[1)] Faculty of Mechanical Engineering, Universiti Teknikal Malaysia Melaka, Hang Tuah Jaya, 76100 Durian Tunggal, Melaka, Malaysia

[2)] Centre for Advanced Research on Energy, Universiti Teknikal Malaysia Melaka, Hang Tuah Jaya, 76100 Durian Tunggal, Melaka, Malaysia,

[*]Corresponding e-mail: mohdazman@utem.edu.my

Keywords: Narrow track vehicle; chassis design; finite element analysis

ABSTRACT – Nowadays traffic problems with traffic congestion and limited highway available, are major concern among drivers. In order to overcome this problem, a more compact vehicle is needed compare to conventional vehicle that being used to ease driving experience hence narrow track vehicle (NTV) is developed. Chassis which is an integral part, act as a structural backbone for any type of vehicle which main function is to provide support to the vehicle and at the same time protect the driver in the cockpit. It is often expose to a dashing environment, hence different type of force and load acting resulting in stress towards the chassis. To ensure the safety of the driver, Finite Element Analysis (FEA) is carried out on the chassis to make sure the chassis does not fail on certain condition. FEA done on this study are static, acceleration, braking and cornering using CATIA V5 software which factor safety will be obtained to ensure the safety of the chassis.

INTRODUCTION

A chassis which supports a man-made object consists of several parts. It is similar to an animal's skeleton where a vehicle without a body is called a chassis. Chassis is considered as backbone of a vehicle thus it is an important feature. It is also one of the most complex structures in vehicle. It provides attachment points for all other major components and manages the stress between them [1]. Chassis also plays an important role in protecting the occupants when accidents happen, where it could reduce the percentage of serious injury [1]. Furthermore it acts as main mounting for other components such as transmission, axel, wheel and etc.

Space frames manufacturing is cheap and damages to the chassis itself can be easily repaired which only requires simple tools [2]. The main benefits of space frame chassis construction are the weight of the structure is less compare to other types of chassis but due to complex manufacturing process, space frame chassis is selected only for high performance and niche market vehicle [3].

The chassis design of this paper will be different than convenient vehicle as the objective of the design is to meet the narrow track vehicle specification. Narrow track vehicle is a vehicle which specially designs to meet certain criteria which is to maneuverer the vehicle in a small space. The compact size of the vehicle enhances the movement of the vehicle in a tight space which fully accommodates the purpose of it. Narrow track vehicle is developed to combat against nowadays traffic problem which is traffic congestion and limited highway available. The chassis need to endure load from the driver and other components to ensure the safety of the vehicle. It also need to clarify whether wheelbase of the vehicle affecting the safety of the factor.

METHODOLOGY

The body tends to rotate on the exact axis as force is exerting at a certain length from an axis. Chassis can be seen as torsional spring as load exert on the suspended wheel as shown in Figure 1. Torsional loading can influence the handling and performance of vehicle hence resulting in momentary elastic or permanent plastic deformation. Stiffness is referred as resistance to torsional deformation which calculated in Nm/degree in SI units. It is important to note that torsional rigidity play a big role in determining performance of vehicle [4,5].

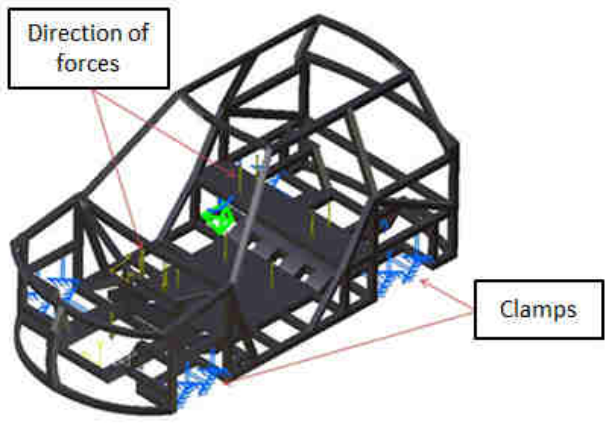

Figure 1 Chassis design and analysis constraints

Major contributors for lateral bending which are forces exert on chassis in result of centrifugal force due to cornering. It is also found that wind produce a significant effect on lateral bending. Lateral forces act along the chassis is supported by the tire, axles, frames, and diagonal hoops [6].

In this study, only the major components that are placed inside the chassis are being considered. These weight components are the weight of the engine and the weight of the driver. The weight of the driver that being

analyzed are 900 N, 1000 N and 1100 N, while weight for engine that being analyzed are 3000 N, 4000 N, and 5000 N for all the 3 chassis. In order to obtain safety factor, the maximum yield strength is divided to the maximum Von Misses stress from the analysis or the maximum allowable stress.

RESULT AND DISCUSSION

Figure 2 shows the Von Mises stress obtained from static analysis of 1.3 m wheelbase with 900 N weight of driver and 3000 N weight of engine which maximum stress obtained was 112 MPa. Maximum stress obtained was used as allowable stress while ultimate stress of material is 250 MPa, which both will be used to calculate safety factor. Safety factor is obtained by dividing ultimate stress of material with allowable stress which produces a value of 2.23. Table 1 summarize the results from the analysis. The Von Misses stress obtained from acceleration analysis with 1100 N weight of driver and 5000 N weight of engine which maximum stress obtained was 186 MPa. The same method of calculation for safety factor produces value of 1.34.

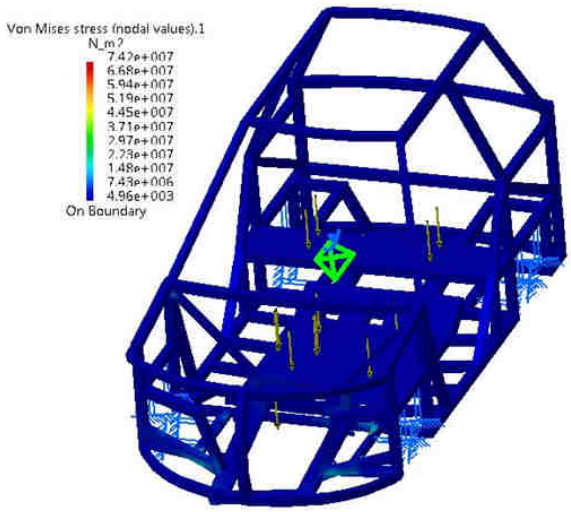

Figure 2 Stress analysis of NTV

Table 1 Cornering analysis results

Driver weight (N)	Engine weight (N)	Total weight (Driver + Engine) (N)	Max Von Mises (N/m^2)	Safety factor
900	3000	3900	1.12×10^8	2.23
	4000	4900	1.49×10^8	1.67
	5000	5900	1.85×10^8	1.35
1000	3000	4000	1.12×10^8	2.23
	4000	5000	1.49×10^8	1.68
	5000	6000	1.85×10^8	1.35
1100	3000	4100	1.12×10^8	2.23
	4000	5100	1.49×10^8	1.67
	5000	6100	1.86×10^8	1.34

CONCLUSION

In conclusion, the design and analysis of NTV chassis are performed. The design is based on 1.3 m wheel base size and 1.0 m track size. The cornering analysis both involve the acting of inertia upon the chassis which backward direction for acceleration and sideway direction for cornering analysis. This inertia will affect the outcome of the force acted on the chassis. Base on the research done the chassis that had been modelled are safe to use as all of them had safety factor of more than 1.3.

ACKNOWLEDGEMENT

The authors gratefully acknowledged the Advanced Vehicle Technology (AcTiVe) research group of Centre for Advanced Research on Energy (CARe), the financial support from Universiti Teknikal Malaysia Melaka and The ministry of Education, Malaysia under Short Term Research Grant, Grant no. PJP/2014/FKM(10A)/S01330 and Fundamental Research Grant Scheme (FRGS), grant no.: FRGS/2013/FKM/TK06/02/2/F00165.

REFERENCES

[1] M.A. Abdullah, S.A. Shamsudin, F.R. Ramli, M.H. Harun and M. A. Yusuff, "Design and fabrication of a recreational human-powered vehicle", *International Journal of Engineering Science Invention (IJESI)*, Vols. 5, No. 2, ISSN (Online): 2319 – 6734, ISSN (Print): 2319 – 6726, 11-14, 2016.

[2] H. Jaiswal, A. Kumar, A. Anand and P. P. Patil "Free Vibration Mode Shape Analysis of Space Frame Chassis of a Sports Car based on FEA", *Proc. of the Intl. Conf. on Advances In Engineering And Technology - ICAET-2014*, pp.330–332, 2014.

[3] M.A.B. Marzuki, M.A. Abu Bakar and M.F. Mohammed Azmi, "Designing Space Frame Race Car Chassis Structure Using Natural Frequencies Data from ANSYS Mode Shape Analysis", *FTMS*, ISSN: 2289-2265, Vol.1, No 1, 2015.

[4] M.A. Abdullah, N. Tamaldin, F.R. Ramli, M.N. Sudin, and A.M. Mohamed Muslim, "Analysis of the Chassis and Components of All Terrain Vehicle (ATV)", *Applied Mechanics and Materials, Trans Tech Publications*, Vols. 660, pp 753-757, doi:10.4028/www.scientific.net/AMM.660.753, 2014.

[5] M.A. Abdullah, M.R. Mansor, M.Mohd Tahir, S.I. Abdul Kudus, M.Z. Hassan and M.N. Ngadiman, "Design, Analysis and Fabrication of Chassis Frame for UTeM Formula VarsityTM Race Car", *International Journal of Mining, Metallurgy & Mechanical Engineering (IJMMME)*, Volume 1, Issue 1, 75-77, ISSN 2320–4060 (Online), 2013.

[6] M.A. Abdullah, A.H. Mohamad and F.R. Ramli, "Design, Analysis and Fabrication of Fixed-Base Driving Simulator Frame", *The Journal of Engineering and Technology (JET)*, Vol 4, No. 2, pp.85-102, 2013.

Proceedings of Innovative Research and Industrial Dialogue'16, pp. 179-180 (May 2017)

Design selection and analysis of human-powered vehicle

M.A. Abdullah[1,2,*], M.Z. Azis[1], M.H. Harun[1,2], F.R. Ramli[1,2] and S. Mat[1,2]

[1)] Faculty of Mechanical Engineering, Universiti Teknikal Malaysia Melaka, Hang Tuah Jaya, 76100 Durian Tunggal, Melaka, Malaysia

[2)] Centre for Advanced Research on Energy, Universiti Teknikal Malaysia Melaka, Hang Tuah Jaya, 76100 Durian Tunggal, Melaka, Malaysia,

[*]Corresponding e-mail: mohdazman@utem.edu.my

Keywords: Human-powered vehicle; design selection; weighted decision matrix

ABSTRACT – This paper presents the design selection and improvement of human powered vehicle (HPV). Three components designs of HPV's are analyzed using CATIA V5 software which are chassis, suspension and hub. The load applied to the chassis is obtained from the weight of driver, the load applied to the suspension is obtained from the total weight of driver and chassis and the load applied to the hub is obtained from total weight of driver, chassis and suspensions. The analysis of these parts produces stress distribution and factor of safety. The HPV that have favorable factor of safety is selected for further improvement.

1. INTRODUCTION

Human Powered Vehicles (HPV) is created to provide people vehicle which is more eco-friendly and energy efficient. HPV can be divided into five sub system. There is chassis, brake, power train, steering and wheels. When design and modeling of HPV, the first thing to do is design the frame or chassis of the vehicle [1]. Human powered vehicle (HPV) is one of the technologies that has been developed and if well designed can be popularized as viable form of sustainable transportation and green technology [1]. In order to build a HPV, there are important components that must be considered. It is chassis, suspension and hub. Chassis is the frame structure of a vehicle [2, 3]. Suspension is the component to provide comfort to driver and a hub is component that centrally located on a wheel. In order to select the chassis design of HPV for improvement, important thing to be considered is safety factor. Safety factor is used to know whether the design structure is safe or not [4].

In this paper, the methodology of this project will be explained in detail about the research methods performed in order to produce an excellent result. Initially, three design of HPV is selected randomly. All the design was undergo several analyses on certain part which is chassis, suspension and hub. The type of analysis used is static analysis [5, 6]. The best design of HPV is selected based on the lowest score in weighted decision matrix.

2. METHODOLOGY

Design analysis is a method to analyze components for safety reason. There are three components of the HPV are analyzed, the chassis, suspension and hub. The analysis used for this stage is static analysis where the HPV is not moved. First analysis is the load from a driver to the chassis. Load of the driver is the weight of driver due to gravity. The load from the driver is a static loading. A static loading analysis is calculated while ignoring inertia and damping effects, such as those caused by time-varying loads. Analysis is done when the driver sits on bicycle and not moving. The mass of driver for every HPV is assumed to be 100 kg. Since the weight is to be evenly distributed to the seat, the support for the seat will receive 981 N of load.

Design selection was done to select which HPV is most suitable to make improvement to its chassis. HPV is selected by calculate its total factor of safety of several part which is chassis, suspension and hub. FEA from CATIA software is used to analyze all the parts of HPV. HPV is selected by the score from factor of safety for each part of HPV. Eqn (1), Eqn (2) and Eqn (3) are used to calculate the score where F_{sci} is the factor of safety for i-number of chassis, F_{ssi} is the factor of safety for i-number of suspension, and F_{shi} is the factor of safety for i-number of hub. HPV that has lowest score is selected as the best design.

$$\text{Chassis score, } S_c = (F_{sci} / \sum F_{sci}) \quad (1)$$

$$\text{Suspension score, } S_s = (F_{ssi} / \sum F_{ssi}) \quad (2)$$

$$\text{Hub score, } S_h = (F_{shi} / \sum F_{shi}) \quad (3)$$

3. RESULTS AND DISCUSSION

Figure 1, 2 and 3 show the sample results from analysis of chassis for all three designs. The value of maximum stress in red in color is used to calculate factor of safety (Table 1) for every part of HPV where the factor of safety is the ratio of material yield strength to the maximum stress. HPV with lowest score is selected (Table 2).

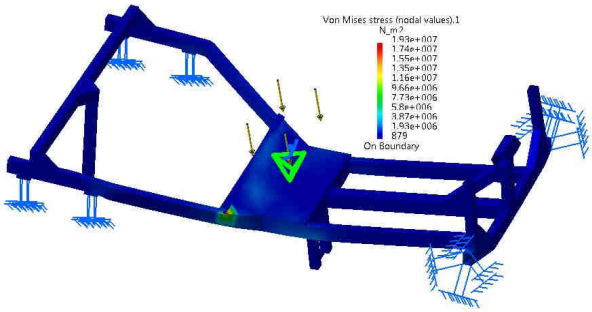

Figure 1 Stress analysis of HPV 1

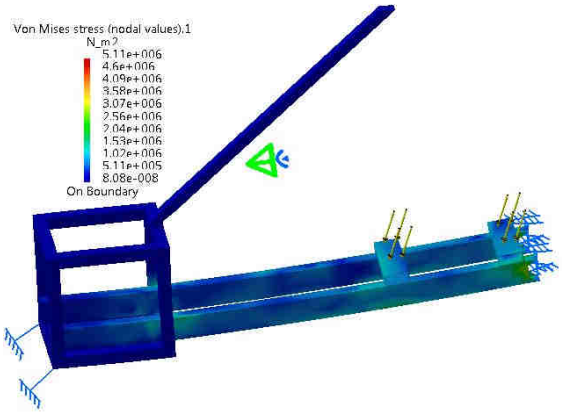

Figure 2 Stress analysis of HPV 2

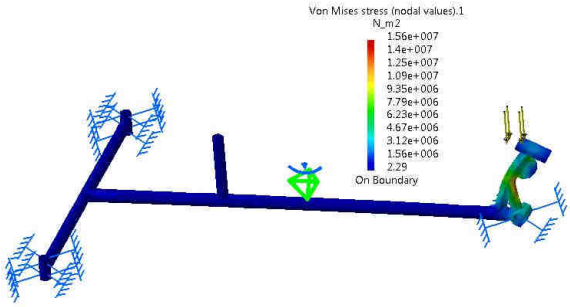

Figure 3 Stress analysis of HPV 3

Table 1 Factor of safety of HPV

Design	HPV 1	HPV 2	HPV 3
F_{sc}	13	28	16
F_{ss}	0.0372	0.0690	0.3771
F_{sh}	98.43	90.25	103.06

Table 2 Total score of HPV

Score	HPV 1	HPV 2	HPV 3
S_c	0.2281	0.4912	0.2807
S_s	0.0770	0.1428	0.7803
S_h	0.2928	0.3519	0.3553
Total Score	0.60	0.99	1.42

4. CONCLUSION

Three number of HPVs designs are randomly selected and undergone stress analysis for their chassis, suspension and hub. The design selection of the HPV is based on the weighted decision matrix score from safety factor of the chassis, suspension and hub. HPV 1 has been selected for further improvement due to the lowest score overall.

ACKNOWLEDGEMENT

The authors gratefully acknowledged the Advanced Vehicle Technology (AcTiVe) research group of Centre for Advanced Research on Energy (CARe), the financial support from Universiti Teknikal Malaysia Melaka and The ministry of Education, Malaysia under Short Term Research Grant, Grant no. PJP/2014/FKM(10A)/S01330 and Fundamental Research Grant Scheme (FRGS), grant no.: FRGS/2013/FKM/TK06/02/2/F00165.

REFERENCES

[1] M.A. Abdullah, S.A. Shamsudin, F.R. Ramli, M.H. Harun, M. A. Yusuff, "Design and fabrication of a recreational human-powered vehicle", *International Journal of Engineering Science Invention (IJESI)*, Vols. 5, No. 2, ISSN (Online): 2319 – 6734, ISSN (Print): 2319 – 6726, 11-14, 2016.

[2] E. Bhaskar, T. Muneiah, and C.V. Rajesh, "Static and Dynamic Analysis of Chassis", *International Journal of Research*, pp.320-328, 2014.

[3] S. Pardeshi and P. Desle, P. "Design and Development of Effective Low Weight Racing Bicycle Frame", *International Journal of Innovative Research in Science, Engineering and Technology,* pp.18215-18221, 2014.

[4] M.A. Abdullah, N. Tamaldin, F.R. Ramli, M.N. Sudin, and A.M. Mohamed Muslim, "Analysis of the Chassis and Components of All Terrain Vehicle (ATV)", *Applied Mechanics and Materials, Trans Tech Publications*, Vols. 660, pp 753-757, doi:10.4028/www.scientific.net/AMM.660.753, 2014.

[5] M.A. Abdullah, M.R. Mansor, M.Mohd Tahir, S.I. Abdul Kudus, M.Z. Hassan and M.N. Ngadiman, "Design, Analysis and Fabrication of Chassis Frame for UTeM Formula VarsityTM Race Car", *International Journal of Mining, Metallurgy & Mechanical Engineering (IJMMME)*, Volume 1, Issue 1, 75-77, ISSN 2320–4060 (Online), 2013.

[6] M.A. Abdullah, A.H. Mohamad and F.R. Ramli, "Design, Analysis and Fabrication of Fixed-Base Driving Simulator Frame", *The Journal of Engineering and Technology (JET)*, Vol 4, No. 2, pp.85-102, 2013.